Science

RESEARCH ARTICLES

Cite as: Y. Zhang *et al.*, *Science*
10.1126/science.aef8874 (2026)

Recovering signatures of archaic hominin introgression using ancestral recombination graphs

Yulin Zhang[1]*†, Arjun Biddanda[2,3]*†, Sarah A. Johnson[1], Colm O'Dushlaine[3]‡, Priya Moorjani[1,4]*

[1]Center for Computational Biology, University of California Berkeley, Berkeley, CA, USA. [2]Department of Biology, Johns Hopkins University, Baltimore, MD, USA. [3]54Gene, Inc. Washington, D.C., USA. [4]Department of Molecular and Cell Biology, University of California Berkeley, Berkeley, CA, USA.

†These authors contributed equally to this work.

‡Present address: insitro Inc. South San Francisco, CA, USA.

***Corresponding author. Email: zhangyulin9806@berkeley.edu (Y.Z.); abiddan1@jhu.edu (A.B.); moorjani@berkeley.edu (P.M.)**

Admixture between modern humans and extinct hominins has shaped the genomes of present-day individuals, but reconstructing this history has been constrained by the scarcity of archaic samples and unadmixed outgroup populations. We introduce TRACE, a reference- and outgroup-free approach that uses features of ancestral recombination graphs to identify archaic ancestry. Simulations show TRACE has high precision and low false discovery rates. Applied to 1000 Genomes, TRACE recovers known Neanderthal and Denisovan introgression and uncovers ghost admixture from uncharacterized hominins in both Africans and non-Africans. Ghost ancestry persists in Neanderthal and Denisovan ancestry deserts, challenging their interpretation as *Homo sapiens*–specific regions. In Oceanians, TRACE finds deep lineages are enriched in Denisovan compared to Neanderthal regions, supporting super-archaic introgression. TRACE enables mapping archaic introgression without archaic genomes.

The sequencing of the Neanderthal and Denisovan genomes has transformed our understanding of human evolution, revealing evidence for gene flow between modern humans and archaic hominins (*1*–*5*). Most non-Africans living today possess 1 to 2% Neanderthal ancestry, and Asians and Oceanians harbor ~0.1 to 5% Denisovan ancestry (*6*, *7*). Archaic ancestry has had a major impact on human adaptation and disease, contributing to a range of traits such as skin pigmentation, high altitude adaptation, and immune function (*8*–*14*). To date, however, only six high-coverage archaic genomes have been published––four Neanderthals and two Denisovan––all from Eurasia. Thus, our knowledge of the evolutionary history and impact of archaic ancestry outside Eurasia and at deeper timescales remains incomplete (*1*–*3*, *5*, *15*, *16*).

Several studies have posited that gene flow from other unknown archaic hominins—for whom no genomic sequences currently exist—may have occurred both within and outside Africa (*17*–*31*). Genetic analyses of present-day African populations have identified highly divergent haplotypes that cannot be explained by known demographic histories, hinting at "ghost" introgression (*17*–*29*, *31*). At deeper timescales, analysis of the Altai Denisovan genome suggests that they harbor ancestry from a deeply divergent population, referred to as "super-archaic," that split from modern humans around 0.9–1.4 million years ago (Mya) (*2*, *3*, *32*). Whereas ghost lineages refer broadly to any unsampled archaic population contributing to modern genomes, super-archaic ancestry specifically denotes contributions from lineages that diverged before the common ancestor of modern humans and Neanderthals/Denisovans. Super-archaic ancestry likely introgressed into modern humans through Denisovan gene flow, and thus may be present in Asians and Oceanians. These histories, however, remain poorly understood as most available methods for studying archaic introgression rely on either sequenced archaic genomes (*33*) or an outgroup population without archaic ancestry (*18*, *34*–*36*), or both (*6*, *37*). As the oldest ancient genome from Africa is less than 20,000 years old (*26*) and recovering hominin DNA older than a million years outside of permafrost is improbable (*38*), methods without such requirements are needed.

With the availability of new methods to reconstruct ancestral recombination graphs (ARGs) (*39*–*42*), it is now possible to infer the full evolutionary history of a set of sequences in a computationally tractable manner. An ARG provides a complete record of all the coalescence and recombination events and specifies a complete genealogy at each position in the genome (*43*–*46*). Importantly, gene flow from deeply divergent lineages is expected to leave distinct signatures in the ARG––such as unusually deep coalescent events––that can be used to detect introgression, even in the absence of archaic reference genomes (*42*).

We introduce TRACE (*TR*acking *A*rchaic *C*ontributions via ARG *E*stimation), a method for identifying footprints of archaic ancestry in modern human genomes by leveraging

features of ARGs constructed from contemporary genomes alone, requiring neither an archaic reference genome nor an unadmixed outgroup population. We perform extensive simulations to characterize the reliability of TRACE under a range of demographic scenarios, using true and inferred ARGs. We then apply TRACE to whole-genome sequences of individuals from worldwide populations to reconstruct the evolutionary history and legacy of archaic gene flow in modern humans.

Results

TRACE identifies archaic gene flow using ancestral recombination graphs

TRACE infers archaic ancestry by leveraging genealogical information encoded in ARGs. The central idea is that archaic introgression leaves two characteristic signatures in the sequence of marginal trees within an ARG: long branches and long haplotypes. First, long branches arise because introgression from a deeply divergent population introduces lineages that coalesce much further back in time than nonintrogressed lineages (*47*). In the ARG, this appears as branches with deep coalescence times that span the interval between the divergence time of the archaic and modern lineages ($T_{archaic}$) and the time of the admixture event (T_{admix}) (Fig. 1A) (*42*). Second, because admixture is more recent than divergence, introgressed segments are expected to be longer than those arising from incomplete lineage sorting (ILS), as less time has elapsed since admixture for recombination to break down the ancestry tracts (*48*).

TRACE is implemented as a hidden Markov model with two states––archaic and modern human. As input, it uses ARGs inferred from phased whole-genome sequences of contemporary individuals. For each marginal tree and focal haplotype, we examine (i) the length of the branch ancestral to the focal sample at time t and (ii) the number of other coalescent events on the tree that fall within the same time window (Fig. 1B and fig. S1). The parameter t—which defines the time cutoff for identifying "long" branches—is specified by the user and represents the proxy for the divergence between the introgressing lineages. The optimal performance of TRACE is achieved when t is close to the true divergence time $T_{archaic}$; if t is set much older than $T_{archaic}$, some true signals may be missed if the introgressed archaic lineage coalesces with modern human lineages before t. Alternatively, if t is set too young, archaic inference results can be sensitive to other recent demographic events (fig. S3).

To validate TRACE, we simulated genome sequences for three populations including Africans, non-Africans and Neanderthals, incorporating an Out-of-Africa (OOA) bottleneck and ~2% Neanderthal gene flow into non-Africans (*22*, *49*). We applied TRACE to detect archaic ancestry in non-Africans using true ARGs for non-Africans (target, $n = 100$) and Africans ($n = 100$). We constructed ARGs jointly across populations to minimize the impact of population bottlenecks on the inference (figs. S2 to S6). Applying $t = 15,000$ generations close to the divergence time between Neanderthals and modern humans (*4*) and focusing on ancestry segments longer than 0.05 centi-Morgan (cM) to distinguish introgressed segments from ILS (*50*), we find TRACE has high (92%) accuracy and high (71%) recall. The false discovery rate is very low (FDR < 0.25%) as shown by applying TRACE to populations without archaic ancestry (Fig. 1C and supplementary section S1.3). Compared with published archaic inference methods *hmmix* (*34*), *Sprime* (*35*) and *IBDmix* (*33*), TRACE does not require a sequenced archaic genome or an unadmixed outgroup. In simulations, we observe that even small amounts of archaic gene flow into the outgroup can bias reference-free methods such as *hmmix* and *Sprime*, whereas TRACE maintains high sensitivity and specificity (fig. S7). Reference-based methods such as IBDmix are not applicable to ghost ancestry inference, and indeed can only recover <0.1% ghost ancestry in simulations (table S8). TRACE shows robust performance across a range of additional demographic models and parameters, including varying proportions of Neanderthal ancestry (0.5–10%), divergence times (~9250 to 24,300 generations), introgression times (725 to 5725 generations), target sample sizes (10 to 200) and misspecification of parameter t (figs. S3 to S8 and supplementary section S2).

Next, we applied TRACE to ARGs inferred using two recently published methods, SINGER (*40*) and *Relate* (*42*). Similar to the performance with true ARGs, TRACE achieves high precision (~90%) and low FDR (<0.25%) using the inferred ARGs (Fig. 1, C and D, and fig. S9). However, the recall is substantially lower with inferred ARGs compared to true ARGs. For the OOA model (fig. S2B), TRACE recovers less than 10% of true segments using *Relate* and approximately 50% using SINGER, compared to around 80% recall using true ARGs (fig. S9). Furthermore, recall decreases under more complex demographic models, though SINGER maintains higher recall (around 30%) than *Relate* under most demographic scenarios (fig. S10). Thus, we applied TRACE to SINGER-inferred ARGs for subsequent analysis of empirical data (supplementary section S3 and figs. S9 to S14).

Evidence of ghost admixture in modern human populations before the Out-of-Africa migration

We analyzed 503 phased whole-genome sequences from the 1000 Genomes Project (1000G) using SINGER reconstructed ARGs (no archaic genomes included).To identify archaic introgression signals, we applied TRACE with $t = 15,000$ generations [or 420,000 years, assuming a generation time of 28

years (*51*)], close to the estimated divergence time between modern humans and Neanderthals (*4*). To minimize the impact of ILS, we retained archaic segments longer than 50 kilobase pairs (kbp) and 0.05 cM (which translates to FDR < 0.2% in simulations, Fig. 1D). We then compared variants on the inferred archaic segments with four high-coverage sequenced archaic genomes [three Neanderthals (*2*, *3*, *5*) and one Denisovan (*1*)] to identify the source of archaic ancestry. For comparison, we also applied *IBDmix* (using the Altai Neanderthal and Altai Denisovan genomes) and *hmmix* (using 426 sub-Saharan Africans as outgroup) (supplementary section S4).

In non-African populations, TRACE identifies 0.8 to 1% Neanderthal ancestry per individual in Europeans, East Asians, and South Asians (Fig. 2A). We recovered minimal Denisovan ancestry in Europeans (0.03%), with higher levels in East and South Asians (0.10% each), consistent with published results (*35*, *52*–*55*). More than 90% of Neanderthal and 70% of Denisovan segments identified by TRACE were also inferred by *hmmix* or *IBDmix* (table S4). In both West and East Africans, TRACE detects less than 0.1% combined Neanderthal and Denisovan ancestry per individual. Around half of the Neanderthal segments identified by TRACE were also inferred by *IBDmix* (table S4, *hmmix* was not applied as there is no reliable outgroup for sub-Saharan Africans). We note that TRACE recovers less total Neanderthal and Denisovan ancestry compared to some previous studies (*33*, *54*, *55*) owing to the lower recall with inferred ARGs, though the recovered segments show no obvious bias relative to those identified by *hmmix* and *IBDmix* (supplementary sections S4.3 and S5.2, table S7, figs. S10, S15, and S16). Nevertheless, TRACE robustly reconstructs the major features of Neanderthal and Denisovan introgression across global populations.

Beyond Neanderthal and Denisovan ancestry, TRACE revealed "ghost" archaic ancestry—introgression from an archaic lineage more distantly related to Neanderthals and Denisovans––in all modern human populations studied. We detected 0.5 to 1.1% of ghost ancestry on average across populations (Fig. 2A). Most ghost ancestry segments found in non-Africans are shared with sub-Saharan Africans, while both East and West Africans harbor a greater diversity of unique ghost segments consistent with the reduction in genetic diversity in non-Africans caused by the OOA bottleneck (Fig. 2B and figs. S23 and S24). Ghost segments exhibit deep divergence in marginal trees and show nearly identical genetic affinity to both sequenced Neanderthal and Denisovan genomes, indicating that they originated from an unsequenced lineage equally related to both archaic groups (Fig. 2C and figs. S17 to S19). The average coalescence time between the ghost and modern human segments, inferred from introgressed segments in the inferred ARGs is approximately 0.83 Mya (95% CI: 0.83 to 0.84 Mya, table S6).

Several additional lines of evidence support our results of ghost ancestry in modern humans. First, we find that genomic regions harboring ghost ancestry exhibit elevated heterozygosity levels, a pattern also observed for Neanderthal and Denisovan segments (fig. S25). The elevation in heterozygosity is consistent with a model of introgression from a deeply divergent lineage (*56*) and importantly, suggests that the ghost ancestry signal is not an artifact of ARG inference. Second, across all tested populations, ghost ancestry segments are shorter than Neanderthal and Denisovan segments, reflecting a more ancient introgression event predating Neanderthal gene flow (fig. S26). Additionally, we validated in simulations that in a model lacking ghost introgression, TRACE infers negligible levels of ghost ancestry (0.07%, 95% CI: 0 to 0.3%), markedly below the estimates from empirical data. By contrast, simulations including a ghost lineage produced results that closely matched empirical observations (tables S7 to S9, figs. S27 and S28, and supplementary section S5). Furthermore, we computed the site frequency spectrum (SFS) and conditional SFS (cSFS) for variants present on archaic segments identified by TRACE (figs. S20 to S22). While Neanderthal and Denisovan segments show the expected "U-shape" (*17*), ghost segments display distinct SFS and cSFS patterns that are consistent with a model of pre–OOA ghost introgression in simulations (fig. S29 and S30).

Together, these findings suggest that an unknown archaic population, which diverged more than 500,000 years ago, introgressed into the common ancestors of all modern humans prior to the OOA migration, resulting in similar patterns of ghost ancestry in non-Africans and Africans.

The landscape of ghost ancestry in modern humans

To explore the legacy of ghost ancestry in modern humans, we examined the genome-wide distribution of ghost ancestry in global populations. Across all ghost haplotypes identified in all populations (sub-Saharan Africans and non-Africans) by TRACE, we recovered 1548.75 Mbp or 71.54% of the accessible genome (Fig. 3, supplementary section S6). Broadly, the genome-wide patterns of ghost ancestry segments resemble those expected from hybridization between deeply divergent lineages (*57*–*59*). We find that ghost ancestry decreases in proximity to functional elements (lower B score (*60*); $\rho_{Spearman} = 0.45,\ p < 2.2\times10^{-308}$) and in regions of low recombination ($\rho_{Spearman} = 0.34,\ p < 2.2\times10^{-308}$), reflecting stronger effects of linked selection in these regions (*61*, *62*). These patterns mimic those seen in Neanderthal and Denisovan introgression maps (*6*, *53*) as well as patterns of hybridization across non-human species (*59*) (fig. S31 and S32, table S10, and supplementary section S6.1).

We also scanned for "peaks" of ghost ancestry, defined as

regions with ghost ancestry frequency greater than 2 standard deviations above the population-specific genome-wide average. Across all tested populations, we identified 1932 peaks of ghost ancestry (average length 61 kbp, SD 64 kbp) (supplementary section S6.2, Fig. 3, and table S13). This result contrasts with the smaller number of 1155 and 160 peaks of Neanderthal and Denisovan ancestry, respectively (average length 84.97 and 76.54 kbp). We find that ghost ancestry peaks are over-represented in sub-Saharan African populations relative to non-African populations, which is consistent with the lower genetic diversity in non-Africans (figs. S33 and S34). Several genes intersect with high-frequency peaks of ghost ancestry, such as *CSMD1* and *RBFOX1*, with an overall functional enrichment for immune and metabolic complexes, including the major histocompatibility and lipoprotein complexes ($p<10^{-5}$ using binomial test; figs. S35 and S36). We also identify 97 deserts of ghost ancestry (i.e., regions that are at least 10 Mbp long and have less than 0.1% frequency of ghost ancestry). These deserts are only found in non-African populations, with nearly half (43.3%) shared between different non-African groups, likely formed during the OOA bottleneck (supplementary section S6.3 and figs. S37 and S38). We do not identify any ghost ancestry deserts in sub-Saharan Africans (though this may depend on the specific frequency and haplotype length thresholds applied). Overall, we find large heterogeneity in the distribution of ghost ancestry tracts across the genome.

Neanderthal and Denisovan deserts are often considered candidates for *Homo sapiens*–specific regions (*63*, *7*). We examined ghost ancestry in five Neanderthal and Denisovan shared deserts identified by two previous studies [figs. S39 to S45, tables S11 and S12, and supplementary section S6.4 (*53*, *7*)]. We replicate the absence of both ancestries in two deserts, but find non-negligible Neanderthal or Denisovan ancestry in some others consistent with recent studies (*7*, *53*, *54*, *63*, *65*). Nevertheless, all five regions contain substantial ghost ancestry, even after restricting to longer and more confidently inferred segments (>100 kbp; Fig. 3B, figs. S39 and S40, and table S11). For example, the shared archaic desert on chromosome 7 containing the *FOXP2* gene has a ghost ancestry peak at 13.3% frequency (Fig. 3B), and the Neanderthal desert on chromosome 3 contains a ghost peak of ~20% frequency overlapping *CSNK2A2IP* (fig. S40). Our findings suggest that ghost ancestry is often present in previously defined archaic deserts, providing additional context to putative *Homo sapiens*–specific selection.

Detecting super-archaic ancestry in Oceanians

Previous studies examining patterns of allele sharing between Neanderthals, Denisovans, and modern humans have suggested Denisovans may harbor ancestry from a super-archaic population (*1*, *2*, *32*). Among modern humans, Oceanians and Southeast Asians derive the highest proportion of Denisovan ancestry (*52*). We therefore reasoned that a fraction of super-archaic ancestry may have been inherited through Denisovan gene flow and may persist within Denisovan-introgressed segments in present-day Oceanians. To test this, we analyzed 92 high-coverage whole-genome sequences from Oceanian individuals including 25 individuals from Papuan New Guinea (*65*) and 67 individuals from Vanuatu and Santa Cruz Islands (*52*). We reconstructed the ARGs using SINGER along with 1000G YRI individuals and applied TRACE with $t = 15,000$ generations to detect archaic ancestry (supplementary section S7.1).

In Oceanian individuals, TRACE inferred an average of 0.73% Neanderthal, 0.66% Denisovan, and 0.33% ghost ancestry (Fig. 4A), lower than estimates from previous studies (*52*) and from other 1000G non-Africans (Fig. 2A and fig. S46). Because Neanderthals and Denisovans coalesce with each other [$t = 13,600 - 16,900$ generations (*2*)] before coalescing with modern humans, many of the long branches are not detected when using $t = 15,000$ generations as the time cutoff. The higher archaic introgression proportion further exacerbates this effect, as a larger fraction of coalescent events occur among archaic lineages (supplementary section S7.2, table S15, and figs. S47 and S57). Simulations mimicking the demographic history of Oceanians replicated this underestimation (supplementary section S8 and tables S15 and S16). Despite lower recall, over 90% of the Neanderthal and Denisovan segments detected by TRACE overlap with those from *hmmix* or *IBDmix* (table S14). Indeed, TRACE-detected archaic segments showed consistent archaic affinity patterns (fig. S48) and site frequency spectra (SFS/cSFS, fig. S49) with 1000G data. Furthermore, ghost segments in Oceanians overlapped with those detected in 1000G populations (fig. S50), consistent with a shared origin in modern humans.

To identify super-archaic introgression, we screened for "super-deep" coalescent events within Denisovan-introgressed segments with $t = 31,500$ generations [inferred divergence time between the super-archaic lineage and modern humans (*32*)], requiring at least 10 kbp and 0.01 cM to distinguish from ILS and applied the same analysis to Neanderthal introgressed segments for comparison. We find a significantly higher proportion of super-deep lineages in Denisovan than in Neanderthal segments ($p<2.2\times10^{-308}$ using binomial test; Fig. 4, supplementary section S7.3). Simulations show that this pattern is inconsistent with a model lacking super-archaic introgression but is recapitulated by a model including super-archaic introgression into Denisovans (Fig. 4C, figs. S56, S58, and S59, and tables S15 to S16). Furthermore, super-archaic fragments within introgressed Denisovan segments exhibit distinct genetic features that

differentiate them from the background Denisovan ancestry, including much deeper coalescence times with modern humans, longer genomic lengths than mean ILS length from Neanderthal deep lineages, and low affinity to both Neanderthal and Denisovan reference genomes (assuming no super-archaic ancestry at the same locus in sequenced Denisovan, supplementary section S8.4, fig. S60, and table S17). Using these features, we detected super-archaic segments in simulations with 70.2% accuracy (95% CI: 66.4 to 74.1%, supplementary section S8.5).

Applied to Oceanian genomes, we infer that the super-archaic segments embedded within Denisovan ancestry tracts range between 20 to 83 kbp (average: 37.6 kbp) and contribute approximately 0.3% of the total detected Denisovan ancestry in Oceanians (table S18 and fig. S51). This estimate constitutes a very conservative lower bound on the true fraction of super-archaic ancestry, as our analysis is restricted to Denisovan-introgressed regions, requires segments of at least 20 kbp, and excludes loci where the sequenced Denisovan carries super-archaic ancestry (figs. S60 and S61 and supplementary section S7.4). We validated that super-archaic segments exhibit higher nucleotide divergence from both modern humans (sub-Saharan Africans) and Altai Denisovans (compared to other Denisovan-introgressed regions), suggesting the signal is not an artifact of ARG inference (fig. S52). Using the marginal trees from SINGER, we estimate the coalescence time between super-archaic and modern human lineages to be approximately 1.77 Mya (95% CI: 1.69 to 1.83 Mya), consistent with earlier reports (*2*, *32*).

We evaluated the potential functional effects of super-archaic segments recovered from Oceanian genomes by characterizing common gene annotations and patterns of functional enrichment (Fig. 4B). Several genic regions harbor high proportions (>70%) of super-archaic tracts such as *RNF39, PPP1R11,* and *POLR1H* within the MHC (Fig. 4B, fig. S53) and *CYP24A1* that is a part of the cytochrome P450 family and a critical regulator of vitamin D degradation in humans (fig. S54) (*30*, *66*–*69*). Gene ontology analysis reveals significant enrichment for several pathways including MHC and activity-related cytoskeleton (ARC), after multiple hypothesis testing (fig. S55).

Discussion

We introduce TRACE, a framework for detecting archaic introgression from ARGs inferred from contemporary genomes alone. TRACE's reference- and outgroup-free design enables the reconstruction of introgression histories that are difficult to resolve with existing approaches, including ghost and super-archaic introgression. As with any ARG-based method, TRACE's performance depends on the accuracy and scalability of the underlying ARG inference, with reduced recall using inferred ARGs relative to ground-truth genealogies. As ARG reconstruction methods continue to advance, the reliability and resolution of TRACE will improve, illuminating episodes of evolutionary history in humans and other species lacking direct genomic references.

Applied to modern human data, TRACE recovers known Neanderthal and Denisovan ancestry and identifies previously uncharacterized signatures of archaic ancestry at varying time points in human history. We find evidence for at least one ghost introgression predating the OOA expansion that contributed ancestry to all present-day populations. This finding is most consistent with a discrete introgression event as in (*17*) but extends that model by showing that the event affected all modern human populations rather than being localized to West Africans. Given that our inferred ghost lineage diverged around the time of the Neanderthal–modern human split (table S6), it represents a more recent event than the proposed deep structure scenarios, involving a population split (>1.5 Mya) followed by later integration through either a single rejoining event around 300 kya (*23*) or multiple "merger" events (*27*). Finally, we infer deeply diverged lineages embedded within Denisovan ancestry in Oceanians, consistent with an additional, indirect contribution from a super-archaic hominin to modern humans. These results point to multiple layers of introgression—both direct and mediated through other archaic groups—shaping modern human genomes.

Beyond the timing and demographic context of these introgression events, their hominin sources remain an open question. Archaeological records document numerous archaic forms with unclear amounts, if any, of potential contribution to modern humans (*30*, *66*, *67*). The ghost lineage, with a divergence time similar to Neanderthals, could plausibly correspond to Middle Pleistocene *Homo* groups (*70*–*72*) or African *Homo heidelbergensis* populations (*73*–*75*) that directly admixed with modern human ancestors before the OOA dispersal. For the super-archaic lineage, one potential candidate—compatible with the split time of approximately 1.8 Mya—is *Homo erectus*, as suggested by earlier studies (*2*, *16*, *32*).

TRACE also illuminates the enduring genomic legacy of archaic ancestry in modern humans. Both ghost and super-archaic ancestry are markedly enriched in functional regions highlighting their role in human adaptation. Moreover, ghost ancestry persists within genomic regions previously identified as deserts of Neanderthal and Denisovan introgression. These deserts have often been interpreted as regions intolerant to archaic introgression due to positive selection for *Homo sapiens*–specific variation or strong purifying selection against archaic introgressed alleles (*57*–*59*). Instead, the persistence of deeply diverged ghost ancestry in these regions suggests lineage-specific selection against Neanderthal and Denisovan introgression, rather than positive selection for

modern-human variation. This pattern implies that differences in genetic load or epistatic incompatibilities associated with Neanderthal and Denisovan lineages––rather than with divergence time alone––shaped Neanderthal and Denisovan ancestry deserts.

Several open questions remain. First, the number, timing, and geographic locations of the inferred ghost introgression events are still uncertain: while our results support at least one pre–OOA introgression event affecting all modern human populations, additional episodes of gene flow among structured African populations may have occurred but remain difficult to resolve with present data. Second, the origin and geographic extent of the super-archaic lineage remains unresolved, including whether this ancestry entered modern humans exclusively via Denisovans or also through direct admixture with ancestors of modern humans. We anticipate that future studies, including new Denisovan reference genomes, may help to further pinpoint the timing and origin of these super-archaic sequences (*75*). Finally, while we detect signatures of selection influencing the distribution of ghost ancestry in the genome, the functional impacts of introgressed archaic regions, including their roles in immunity and metabolism, have yet to be fully characterized. Future studies that integrate additional ancient genomes at deep timescales, particularly from Africa and Asia, will be critical for refining the timing, sources, and evolutionary consequences of these introgression events.

Materials and methods are available in Supplementary Materials.

REFERENCES AND NOTES

1. M. Meyer, M. Kircher, M.-T. Gansauge, H. Li, F. Racimo, S. Mallick, J. G. Schraiber, F. Jay, K. Prüfer, C. de Filippo, P. H. Sudmant, C. Alkan, Q. Fu, R. Do, N. Rohland, A. Tandon, M. Siebauer, R. E. Green, K. Bryc, A. W. Briggs, U. Stenzel, J. Dabney, J. Shendure, J. Kitzman, M. F. Hammer, M. V. Shunkov, A. P. Derevianko, N. Patterson, A. M. Andrés, E. E. Eichler, M. Slatkin, D. Reich, J. Kelso, S. Pääbo, A high-coverage genome sequence from an archaic Denisovan individual. *Science* **338**, 222–226 (2012). doi:10.1126/science.1224344 Medline
2. K. Prüfer, F. Racimo, N. Patterson, F. Jay, S. Sankararaman, S. Sawyer, A. Heinze, G. Renaud, P. H. Sudmant, C. de Filippo, H. Li, S. Mallick, M. Dannemann, Q. Fu, M. Kircher, M. Kuhlwilm, M. Lachmann, M. Meyer, M. Ongyerth, M. Siebauer, C. Theunert, A. Tandon, P. Moorjani, J. Pickrell, J. C. Mullikin, S. H. Vohr, R. E. Green, I. Hellmann, P. L. F. Johnson, H. Blanche, H. Cann, J. O. Kitzman, J. Shendure, E. E. Eichler, E. S. Lein, T. E. Bakken, L. V. Golovanova, V. B. Doronichev, M. V. Shunkov, A. P. Derevianko, B. Viola, M. Slatkin, D. Reich, J. Kelso, S. Pääbo, The complete genome sequence of a Neanderthal from the Altai Mountains. *Nature* **505**, 43–49 (2014). doi:10.1038/nature12886 Medline
3. K. Prüfer, C. de Filippo, S. Grote, F. Mafessoni, P. Korlević, M. Hajdinjak, B. Vernot, L. Skov, P. Hsieh, S. Peyrégne, D. Reher, C. Hopfe, S. Nagel, T. Maricic, Q. Fu, C. Theunert, R. Rogers, P. Skoglund, M. Chintalapati, M. Dannemann, B. J. Nelson, F. M. Key, P. Rudan, Ž. Kucan, I. Gušic, L. V. Golovanova, V. B. Doronichev, N. Patterson, D. Reich, E. E. Eichler, M. Slatkin, M. H. Schierup, A. M. Andrés, J. Kelso, M. Meyer, S. Pääbo, A high-coverage Neandertal genome from Vindija Cave in Croatia. *Science* **358**, 655–658 (2017). doi:10.1126/science.aao1887 Medline
4. R. E. Green, J. Krause, A. W. Briggs, T. Maricic, U. Stenzel, M. Kircher, N. Patterson, H. Li, W. Zhai, M. H.-Y. Fritz, N. F. Hansen, E. Y. Durand, A.-S. Malaspinas, J. D. Jensen, T. Marques-Bonet, C. Alkan, K. Prüfer, M. Meyer, H. A. Burbano, J. M. Good, R. Schultz, A. Aximu-Petri, A. Butthof, B. Höber, B. Höffner, M. Siegemund, A. Weihmann, C. Nusbaum, E. S. Lander, C. Russ, N. Novod, J. Affourtit, M. Egholm, C. Verna, P. Rudan, D. Brajkovic, Ž. Kucan, I. Gušic, V. B. Doronichev, L. V. Golovanova, C. Lalueza-Fox, M. de la Rasilla, J. Fortea, A. Rosas, R. W. Schmitz, P. L. F. Johnson, E. E. Eichler, D. Falush, E. Birney, J. C. Mullikin, M. Slatkin, R. Nielsen, J. Kelso, M. Lachmann, D. Reich, S. Pääbo, A draft sequence of the Neandertal genome. *Science* **328**, 710–722 (2010). doi:10.1126/science.1188021 Medline
5. F. Mafessoni, S. Grote, C. de Filippo, V. Slon, K. A. Kolobova, B. Viola, S. V. Markin, M. Chintalapati, S. Peyrégne, L. Skov, P. Skoglund, A. I. Krivoshapkin, A. P. Derevianko, M. Meyer, J. Kelso, B. Peter, K. Prüfer, S. Pääbo, A high-coverage Neandertal genome from Chagyrskaya Cave. *Proc. Natl. Acad. Sci. U.S.A.* **117**, 15132–15136 (2020). doi:10.1073/pnas.2004944117 Medline
6. S. Sankararaman, S. Mallick, M. Dannemann, K. Prüfer, J. Kelso, S. Pääbo, N. Patterson, D. Reich, The genomic landscape of Neanderthal ancestry in present-day humans. *Nature* **507**, 354–357 (2014). doi:10.1038/nature12961 Medline
7. B. Vernot, S. Tucci, J. Kelso, J. G. Schraiber, A. B. Wolf, R. M. Gittelman, M. Dannemann, S. Grote, R. C. McCoy, H. Norton, L. B. Scheinfeldt, D. A. Merriwether, G. Koki, J. S. Friedlaender, J. Wakefield, S. Pääbo, J. M. Akey, Excavating Neandertal and Denisovan DNA from the genomes of Melanesian individuals. *Science* **352**, 235–239 (2016). doi:10.1126/science.aad9416 Medline
8. F. Racimo, S. Sankararaman, R. Nielsen, E. Huerta-Sánchez, Evidence for archaic adaptive introgression in humans. *Nat. Rev. Genet.* **16**, 359–371 (2015). doi:10.1038/nrg3936 Medline
9. A. J. Sams, A. Dumaine, Y. Nédélec, V. Yotova, C. Alfieri, J. E. Tanner, P. W. Messer, L. B. Barreiro, Adaptively introgressed Neandertal haplotype at the OAS locus functionally impacts innate immune responses in humans. *Genome Biol.* **17**, 246 (2016). doi:10.1186/s13059-016-1098-6 Medline
10. M. Dannemann, J. Kelso, The Contribution of Neanderthals to Phenotypic Variation in Modern Humans. *Am. J. Hum. Genet.* **101**, 578–589 (2017). doi:10.1016/j.ajhg.2017.09.010 Medline
11. E. Huerta-Sánchez, X. Jin, Z. Asan, Z. Bianba, B. M. Peter, N. Vinckenbosch, Y. Liang, X. Yi, M. He, M. Somel, P. Ni, B. Wang, X. Ou, Huasang, J. Luosang, Z. X. Cuo, K. Li, G. Gao, Y. Yin, W. Wang, X. Zhang, X. Xu, H. Yang, Y. Li, J. Wang, J. Wang, R. Nielsen, Altitude adaptation in Tibetans caused by introgression of Denisovan-like DNA. *Nature* **512**, 194–197 (2014). Medline
12. X. Wei, C. R. Robles, A. Pazokitoroudi, A. Ganna, A. Gusev, A. Durvasula, S. Gazal, P.-R. Loh, D. Reich, S. Sankararaman, The lingering effects of Neanderthal introgression on human complex traits. *eLife* **12**, e80757 (2023). doi:10.7554/eLife.80757 Medline
13. H. Zeberg, S. Pääbo, The major genetic risk factor for severe COVID-19 is inherited from Neanderthals. *Nature* **587**, 610–612 (2020). doi:10.1038/s41586-020-2818-3 Medline
14. F. L. Mendez, J. C. Watkins, M. F. Hammer, Neandertal origin of genetic variation at the cluster of OAS immunity genes. *Mol. Biol. Evol.* **30**, 798–801 (2013). doi:10.1093/molbev/mst004 Medline
15. D. Massilani, S. Peyrégne, L. N. M. Iasi, C. de Filippo, F. Mafessoni, A. Bossoms Mesa, A. P. Sümer, Y. Swiel, D. Popli, S. Silverman, M. J. Boyle, M. B. Kozlikin, M. V. Shunkov, A. P. Derevianko, T. Higham, K. Douka, M. Meyer, H. Zeberg, J. Kelso, S. Pääbo, A high-coverage Neandertal genome from the Altai Mountains reveals population structure among Neandertals. *Proc. Natl. Acad. Sci. U.S.A.* **123**, e2534576123 (2026). doi:10.1073/pnas.2534576123 Medline
16. S. Peyrégne, D. Massilani, Y. Swiel, M. J. Boyle, L. N. M. Iasi, A. P. Sümer, A. B. Mesa, C. de Filippo, B. Viola, E. Essel, S. Nagel, J. Richter, A. Weihmann, B. Schellbach, H. Zeberg, J. Visagie, M. B. Kozlikin, M. V. Shunkov, A. P. Derevianko, K. Prüfer, B. M. Peter, M. Meyer, S. Pääbo, J. Kelso, A high-coverage genome from a 200,000-year-old Denisovan, *bioRxiv* (2025). https://www.biorxiv.org/content/10.1101/2025.10.20.683404v1.
17. A. Durvasula, S. Sankararaman, Recovering signals of ghost archaic introgression in African populations. *Sci. Adv.* **6**, eaax5097 (2020). doi:10.1126/sciadv.aax5097 Medline
18. V. Plagnol, J. D. Wall, Possible ancestral structure in human populations. *PLOS Genet.* **2**, e105 (2006). doi:10.1371/journal.pgen.0020105 Medline
19. J. D. Wall, A. Ratan, E. Stawiski, J. D. Wall, E. Stawiski, A. Ratan, H. L. Kim, C. Kim, R. Gupta, K. Suryamohan, E. S. GUSA.reva, R. W. Purbojati, T. Bhangale, V.

Stepanov, V. Kharkov, M. S. Schröder, V. Ramprasad, J. Tom, S. Durinck, Q. Bei, J. Li, J. Guillory, S. Phalke, A. Basu, J. Stinson, S. Nair, S. Malaichamy, N. K. Biswas, J. C. Chambers, K. C. Cheng, J. T. George, S. S. Khor, J.-I. Kim, B. Cho, R. Menon, T. Sattibabu, A. Bassi, M. Deshmukh, A. Verma, V. Gopalan, J.-Y. Shin, M. Pratapneni, S. Santhosh, K. Tokunaga, B. M. Md-Zain, K. G. Chan, M. Parani, P. Natarajan, M. Hauser, R. R. Allingham, C. Santiago-Turla, A. Ghosh, S. G. K. Gadde, C. Fuchsberger, L. Forer, S. Shoenherr, H. Sudoyo, J. S. Lansing, J. Friedlaender, G. Koki, M. P. Cox, M. Hammer, T. Karafet, K. C. Ang, S. Q. Mehdi, V. Radha, V. Mohan, P. P. Majumder, S. Seshagiri, J.-S. Seo, S. Schuster, A. S. Peterson; GenomeAsia 100K Consortium, Identification of African-Specific Admixture between Modern and Archaic Humans. *Am. J. Hum. Genet.* **105**, 1254–1261 (2019). doi:10.1016/j.ajhg.2019.11.005 Medline

20. M. F. Hammer, A. E. Woerner, F. L. Mendez, J. C. Watkins, J. D. Wall, Genetic evidence for archaic admixture in Africa. *Proc. Natl. Acad. Sci. U.S.A.* **108**, 15123–15128 (2011). doi:10.1073/pnas.1109300108 Medline
21. J. Hey, Y. Chung, A. Sethuraman, J. Lachance, S. Tishkoff, V. C. SoUSA., Y. Wang, Phylogeny estimation by integration over Isolation with Migration models. *Mol. Biol. Evol.* **35**, 2805–2818 (2018). doi:10.1093/molbev/msy162 Medline
22. A. P. Ragsdale, S. Gravel, Models of archaic admixture and recent history from two-locus statistics. *PLOS Genet.* **15**, e1008204 (2019). doi:10.1371/journal.pgen.1008204 Medline
23. A. P. Ragsdale, T. D. Weaver, E. G. Atkinson, E. G. Hoal, M. Möller, B. M. Henn, S. Gravel, A weakly structured stem for human origins in Africa. *Nature* **617**, 755–763 (2023). doi:10.1038/s41586-023-06055-y Medline
24. J. Lachance, B. Vernot, C. C. Elbers, B. Ferwerda, A. Froment, J.-M. Bodo, G. Lema, W. Fu, T. B. Nyambo, T. R. Rebbeck, K. Zhang, J. M. Akey, S. A. Tishkoff, Evolutionary history and adaptation from high-coverage whole-genome sequences of diverse African hunter-gatherers. *Cell* **150**, 457–469 (2012). doi:10.1016/j.cell.2012.07.009 Medline
25. P. Hsieh, A. E. Woerner, J. D. Wall, J. Lachance, S. A. Tishkoff, R. N. Gutenkunst, M. F. Hammer, Model-based analyses of whole-genome data reveal a complex evolutionary history involving archaic introgression in Central African Pygmies. *Genome Res.* **26**, 291–300 (2016). doi:10.1101/gr.196634.115 Medline
26. M. Lipson, E. A. Sawchuk, J. C. Thompson, J. Oppenheimer, C. A. Tryon, K. L. Ranhorn, K. M. de Luna, K. A. Sirak, I. Olalde, S. H. Ambrose, J. W. Arthur, K. J. W. Arthur, G. Ayodo, A. Bertacchi, J. I. Cerezo-Román, B. J. Culleton, M. C. Curtis, J. Davis, A. O. Gidna, A. Hanson, P. Kaliba, M. Katongo, A. Kwekason, M. F. Laird, J. Lewis, A. Z. P. Mabulla, F. Mapemba, A. Morris, G. Mudenda, R. Mwafulirwa, D. Mwangomba, E. Ndiema, C. Ogola, F. Schilt, P. R. Willoughby, D. K. Wright, A. Zipkin, R. Pinhasi, D. J. Kennett, F. K. Manthi, N. Rohland, N. Patterson, D. Reich, M. E. Prendergast, Ancient DNA and deep population structure in sub-Saharan African foragers. *Nature* **603**, 290–296 (2022). doi:10.1038/s41586-022-04430-9 Medline
27. T. Cousins, A. Scally, R. Durbin, A structured coalescent model reveals deep ancestral structure shared by all modern humans. *Nat. Genet.* **57**, 856–864 (2025). doi:10.1038/s41588-025-02117-1 Medline
28. P. Skoglund, J. C. Thompson, M. E. Prendergast, A. Mittnik, K. Sirak, M. Hajdinjak, T. Salie, N. Rohland, S. Mallick, A. Peltzer, A. Heinze, I. Olalde, M. Ferry, E. Harney, M. Michel, K. Stewardson, J. I. Cerezo-Román, C. Chiumia, A. Crowther, E. Gomani-Chindebvu, A. O. Gidna, K. M. Grillo, I. T. Helenius, G. Hellenthal, R. Helm, M. Horton, S. Lopez, A. Z. P. Mabulla, J. Parkington, C. Shipton, M. G. Thomas, R. Tibesasa, M. Welling, V. M. Hayes, D. J. Kennett, R. Ramesar, M. Meyer, S. Pääbo, N. Patterson, A. G. Morris, N. Boivin, R. Pinhasi, J. Krause, D. Reich, Reconstructing prehistoric African population structure. *Cell* **171**, 59–71.e21 (2017). doi:10.1016/j.cell.2017.08.049 Medline
29. B. Lorente-Galdos, O. Lao, G. Serra-Vidal, G. Santpere, L. F. K. Kuderna, L. R. Arauna, K. Fadhlaoui-Zid, V. N. Pimenoff, H. Soodyall, P. Zalloua, T. Marques-Bonet, D. Comas, Whole-genome sequence analysis of a Pan African set of samples reveals archaic gene flow from an extinct basal population of modern humans into sub-Saharan populations. *Genome Biol.* **20**, 77 (2019). doi:10.1186/s13059-019-1684-5 Medline
30. E. M. L. Scerri, M. G. Thomas, A. Manica, P. Gunz, J. T. Stock, C. Stringer, M. Grove, H. S. Groucutt, A. Timmermann, G. P. Rightmire, F. d'Errico, C. A. Tryon, N. A. Drake, A. S. Brooks, R. W. Dennell, R. Durbin, B. M. Henn, J. Lee-Thorp, P. deMenocal, M. D. Petraglia, J. C. Thompson, A. Scally, L. Chikhi, Did our species evolve in subdivided populations across Africa, and why does it matter? *Trends Ecol. Evol.* **33**, 582–594 (2018). doi:10.1016/j.tree.2018.05.005 Medline
31. S. Fan, J. P. Spence, Y. Feng, M. E. B. Hansen, J. Terhorst, M. H. Beltrame, A. Ranciaro, J. Hirbo, W. Beggs, N. Thomas, T. Nyambo, S. W. Mpoloka, G. G. Mokone, A. Njamnshi, C. Folkunang, D. W. Meskel, G. Belay, Y. S. Song, S. A. Tishkoff, Whole-genome sequencing reveals a complex African population demographic history and signatures of local adaptation. *Cell* **186**, 923–939.e14 (2023). doi:10.1016/j.cell.2023.01.042 Medline
32. M. J. Hubisz, A. L. Williams, A. Siepel, Mapping gene flow between ancient hominins through demography-aware inference of the ancestral recombination graph. *PLOS Genet.* **16**, e1008895 (2020). doi:10.1371/journal.pgen.1008895 Medline
33. L. Chen, A. B. Wolf, W. Fu, L. Li, J. M. Akey, Identifying and interpreting apparent Neanderthal ancestry in African individuals. *Cell* **180**, 677–687.e16 (2020). doi:10.1016/j.cell.2020.01.012 Medline
34. L. Skov, R. Hui, V. Shchur, A. Hobolth, A. Scally, M. H. Schierup, R. Durbin, Detecting archaic introgression using an unadmixed outgroup. *PLOS Genet.* **14**, e1007641 (2018). doi:10.1371/journal.pgen.1007641 Medline
35. S. R. Browning, B. L. Browning, Y. Zhou, S. Tucci, J. M. Akey, Analysis of human sequence data reveals two pulses of archaic Denisovan admixture. *Cell* **173**, 53–61.e9 (2018). doi:10.1016/j.cell.2018.02.031 Medline
36. A. Durvasula, S. Sankararaman, A statistical model for reference-free inference of archaic local ancestry. *PLOS Genet.* **15**, e1008175 (2019). doi:10.1371/journal.pgen.1008175 Medline
37. M. Steinrücken, J. P. Spence, J. A. Kamm, E. Wieczorek, Y. S. Song, Model-based detection and analysis of introgressed Neanderthal ancestry in modern humans. *Mol. Ecol.* **27**, 3873–3888 (2018). doi:10.1111/mec.14565 Medline
38. L. Orlando, A. Ginolhac, G. Zhang, D. Froese, A. Albrechtsen, M. Stiller, M. Schubert, E. Cappellini, B. Petersen, I. Moltke, P. L. F. Johnson, M. Fumagalli, J. T. Vilstrup, M. Raghavan, T. Korneliussen, A.-S. Malaspinas, J. Vogt, D. Szklarczyk, C. D. Kelstrup, J. Vinther, A. Dolocan, J. Stenderup, A. M. V. Velazquez, J. Cahill, M. Rasmussen, X. Wang, J. Min, G. D. Zazula, A. Seguin-Orlando, C. Mortensen, K. Magnussen, J. F. Thompson, J. Weinstock, K. Gregersen, K. H. Røed, V. Eisenmann, C. J. Rubin, D. C. Miller, D. F. Antczak, M. F. Bertelsen, S. Brunak, K. A. S. Al-Rasheid, O. Ryder, L. Andersson, J. Mundy, A. Krogh, M. T. P. Gilbert, K. Kjær, T. Sicheritz-Ponten, L. J. Jensen, J. V. Olsen, M. Hofreiter, R. Nielsen, B. Shapiro, J. Wang, E. Willerslev, Recalibrating Equus evolution using the genome sequence of an early Middle Pleistocene horse. *Nature* **499**, 74–78 (2013). doi:10.1038/nature12323 Medline
39. J. Kelleher, Y. Wong, A. W. Wohns, C. Fadil, P. K. Albers, G. McVean, Inferring whole-genome histories in large population datasets. *Nat. Genet.* **51**, 1330–1338 (2019). doi:10.1038/s41588-019-0483-y Medline
40. Y. Deng, R. Nielsen, Y. S. Song, Robust and accurate Bayesian inference of genome-wide genealogies for hundreds of genomes. *Nat. Genet.* **57**, 2124–2135 (2025). doi:10.1038/s41588-025-02317-9 Medline
41. M. D. Rasmussen, M. J. Hubisz, I. Gronau, A. Siepel, Genome-wide inference of ancestral recombination graphs. *PLOS Genet.* **10**, e1004342 (2014). doi:10.1371/journal.pgen.1004342 Medline
42. L. Speidel, M. Forest, S. Shi, S. R. Myers, A method for genome-wide genealogy estimation for thoUSA.nds of samples. *Nat. Genet.* **51**, 1321–1329 (2019). doi:10.1038/s41588-019-0484-x Medline
43. R. C. Griffiths, Neutral two-locus multiple allele models with recombination. *Theor. Popul. Biol.* **19**, 169–186 (1981). doi:10.1016/0040-5809(81)90016-2
44. R. R. Hudson, Properties of a neutral allele model with intragenic recombination. *Theor. Popul. Biol.* **23**, 183–201 (1983). doi:10.1016/0040-5809(83)90013-8 Medline
45. D. Y C Brandt, X. Wei, Y. Deng, A. H. Vaughn, R. Nielsen, Evaluation of methods for estimating coalescence times using ancestral recombination graphs. *Genetics* **221**, iyac044 (2022). doi:10.1093/genetics/iyac044 Medline
46. R. Nielsen, A. H. Vaughn, Y. Deng, Inference and applications of ancestral recombination graphs. *Nat. Rev. Genet.* **26**, 47–58 (2025). doi:10.1038/s41576-024-00772-4 Medline
47. M. S. Hibbins, M. W. Hahn, Phylogenomic approaches to detecting and characterizing introgression. *Genetics* **220**, iyab173 (2022). doi:10.1093/genetics/iyab173 Medline
48. P.-R. Loh, M. Lipson, N. Patterson, P. Moorjani, J. K. Pickrell, D. Reich, B. Berger,

Inferring admixture histories of human populations using linkage disequilibrium. *Genetics* **193**, 1233–1254 (2013). doi:10.1534/genetics.112.147330 Medline
49. F. Baumdicker, G. Bisschop, D. Goldstein, G. Gower, A. P. Ragsdale, G. Tsambos, S. Zhu, B. Eldon, E. C. Ellerman, J. G. Galloway, A. L. Gladstein, G. Gorjanc, B. Guo, B. Jeffery, W. W. Kretzschumar, K. Lohse, M. Matschiner, D. Nelson, N. S. Pope, C. D. Quinto-Cortés, M. F. Rodrigues, K. Saunack, T. Sellinger, K. Thornton, H. van Kemenade, A. W. Wohns, Y. Wong, S. Gravel, A. D. Kern, J. Koskela, P. L. Ralph, J. Kelleher, Efficient ancestry and mutation simulation with msprime 1.0. *Genetics* **220**, iyab229 (2022). doi:10.1093/genetics/iyab229 Medline
50. S. Sankararaman, N. Patterson, H. Li, S. Pääbo, D. Reich, The date of interbreeding between Neandertals and modern humans. *PLOS Genet.* **8**, e1002947 (2012). doi:10.1371/journal.pgen.1002947 Medline
51. P. Moorjani, S. Sankararaman, Q. Fu, M. Przeworski, N. Patterson, D. Reich, A genetic method for dating ancient genomes provides a direct estimate of human generation interval in the last 45,000 years. *Proc. Natl. Acad. Sci. U.S.A.* **113**, 5652–5657 (2016). doi:10.1073/pnas.1514696113 Medline
52. J. Choin, J. Mendoza-Revilla, L. R. Arauna, S. Cuadros-Espinoza, O. Cassar, M. Larena, A. M.-S. Ko, C. Harmant, R. Laurent, P. Verdu, G. Laval, A. Boland, R. Olaso, J.-F. Deleuze, F. Valentin, Y.-C. Ko, M. Jakobsson, A. Gessain, L. Excoffier, M. Stoneking, E. Patin, L. Quintana-Murci, Genomic insights into population history and biological adaptation in Oceania. *Nature* **592**, 583–589 (2021). doi:10.1038/s41586-021-03236-5 Medline
53. S. Sankararaman, S. Mallick, N. Patterson, D. Reich, The combined landscape of Denisovan and Neanderthal ancestry in present-day humans. *Curr. Biol.* **26**, 1241–1247 (2016). doi:10.1016/j.cub.2016.03.037 Medline
54. E. Kerdoncuff, L. Skov, N. Patterson, J. Banerjee, P. Khobragade, S. S. Chakrabarti, A. Chakrawarty, P. Chatterjee, M. Dhar, M. Gupta, J. P. John, P. A. Koul, S. S. Lehl, R. R. Mohanty, M. Padmaja, A. Perianayagam, C. Rajguru, L. Sankhe, A. Talukdar, M. Varghese, S. R. Yadati, W. Zhao, Y. Y. Leung, G. D. Schellenberg, Y. Z. Wang, J. A. Smith, S. Dey, A. Ganna, A. B. Dey, S. L. R. Kardia, J. Lee, P. Moorjani, 50,000 years of evolutionary history of India: Impact on health and disease variation. *Cell* **188**, 3389–3404.e6 (2025). doi:10.1016/j.cell.2025.04.027 Medline
55. L. Skov, M. Coll Macià, G. Sveinbjörnsson, F. Mafessoni, E. A. Lucotte, M. S. Einarsdóttir, H. Jonsson, B. Halldorsson, D. F. Gudbjartsson, A. Helgason, M. H. Schierup, K. Stefansson, The nature of Neanderthal introgression revealed by 27,566 Icelandic genomes. *Nature* **582**, 78–83 (2020). doi:10.1038/s41586-020-2225-9 Medline
56. L. Li, T. J. Comi, R. F. Bierman, J. M. Akey, Recurrent gene flow between Neanderthals and modern humans over the past 200,000 years. *Science* **385**, eadi1768 (2024).
57. I. Juric, S. Aeschbacher, G. Coop, The strength of selection against Neanderthal introgression. *PLOS Genet.* **12**, e1006340 (2016). doi:10.1371/journal.pgen.1006340 Medline
58. K. Harris, R. Nielsen, The genetic cost of Neanderthal introgression. *Genetics* **203**, 881–891 (2016). doi:10.1534/genetics.116.186890 Medline
59. B. M. Moran, C. Payne, Q. Langdon, D. L. Powell, Y. Brandvain, M. Schumer, The genomic consequences of hybridization. *eLife* **10**, e69016 (2021). doi:10.7554/eLife.69016 Medline
60. G. McVicker, D. Gordon, C. Davis, P. Green, Widespread genomic signatures of natural selection in hominid evolution. *PLOS Genet.* **5**, e1000471 (2009). doi:10.1371/journal.pgen.1000471 Medline
61. S. Myers, L. Bottolo, C. Freeman, G. McVean, P. Donnelly, A fine-scale map of recombination rates and hotspots across the human genome. *Science* **310**, 321–324 (2005). doi:10.1126/science.1117196 Medline
62. G. Coop, X. Wen, C. Ober, J. K. Pritchard, M. Przeworski, High-resolution mapping of crossovers reveals extensive variation in fine-scale recombination patterns among humans. *Science* **319**, 1395–1398 (2008). doi:10.1126/science.1151851 Medline
63. A. B. Wolf, J. M. Akey, Outstanding questions in the study of archaic hominin admixture. *PLOS Genet.* **14**, e1007349 (2018). doi:10.1371/journal.pgen.1007349 Medline
64. L. N. M. Iasi, M. Chintalapati, L. Skov, A. B. Mesa, M. Hajdinjak, B. M. Peter, P. Moorjani, Neanderthal ancestry through time: Insights from genomes of ancient and present-day humans. *Science* **386**, eadq3010 (2024). doi:10.1126/science.adq3010 Medline
65. A.-S. Malaspinas, M. C. Westaway, C. Muller, V. C. SoUSA., O. Lao, I. Alves, A. Bergström, G. Athanasiadis, J. Y. Cheng, J. E. Crawford, T. H. Heupink, E. Macholdt, S. Peischl, S. Rasmussen, S. Schiffels, S. Subramanian, J. L. Wright, A. Albrechtsen, C. Barbieri, I. Dupanloup, A. Eriksson, A. Margaryan, I. Moltke, I. Pugach, T. S. Korneliussen, I. P. Levkivskyi, J. V. Moreno-Mayar, S. Ni, F. Racimo, M. Sikora, Y. Xue, F. A. Aghakhanian, N. Brucato, S. Brunak, P. F. Campos, W. Clark, S. Ellingvåg, G. Fourmile, P. Gerbault, D. Injie, G. Koki, M. Leavesley, B. Logan, A. Lynch, E. A. Matisoo-Smith, P. J. McAllister, A. J. Mentzer, M. Metspalu, A. B. Migliano, L. Murgha, M. E. Phipps, W. Pomat, D. Reynolds, F.-X. Ricaut, P. Siba, M. G. Thomas, T. Wales, C. M. Wall, S. J. Oppenheimer, C. Tyler-Smith, R. Durbin, J. Dortch, A. Manica, M. H. Schierup, R. A. Foley, M. M. Lahr, C. Bowern, J. D. Wall, T. Mailund, M. Stoneking, R. Nielsen, M. S. Sandhu, L. Excoffier, D. M. Lambert, E. Willerslev, A genomic history of Aboriginal Australia. *Nature* **538**, 207–214 (2016). doi:10.1038/nature18299 Medline
66. E. Y. Hallett, M. Leonardi, J. N. Cerasoni, M. Will, R. Beyer, M. Krapp, A. W. Kandel, A. Manica, E. M. L. Scerri, Major expansion in the human niche preceded out of Africa dispersal. *Nature* **644**, 115–121 (2025). doi:10.1038/s41586-025-09154-0 Medline
67. E. Armstrong, M. Tallavaara, P. O. Hopcroft, P. J. Valdes, North African humid periods over the past 800,000 years. *Nat. Commun.* **14**, 5549 (2023). doi:10.1038/s41467-023-41219-4 Medline
68. D. R. Nelson, The cytochrome p450 homepage. *Hum. Genomics* **4**, 59–65 (2009). doi:10.1186/1479-7364-4-1-59 Medline
69. G. Jones, D. E. Prosser, M. Kaufmann, Cytochrome P450-mediated metabolism of vitamin D. *J. Lipid Res.* **55**, 13–31 (2014). doi:10.1194/jlr.R031534 Medline
70. M. Roksandic, P. Radović, X.-J. Wu, C. J. Bae, Resolving the "muddle in the middle": The case for Homo bodoensis sp. nov. *Evol. Anthropol.* **31**, 20–29 (2022). doi:10.1002/evan.21929 Medline
71. W. B. Reiner, F. Masao, S. B. Sholts, A. V. Songita, I. Stanistreet, H. Stollhofen, R. E. Taylor, L. J. Hlusko, OH 83: A new early modern human fossil cranium from the Ndutu beds of Olduvai Gorge, Tanzania. *Am. J. Phys. Anthropol.* **164**, 533–545 (2017). doi:10.1002/ajpa.23292 Medline
72. A. A. Mturi, New hominid from lake ndutu, Tanzania. *Nature* **262**, 484–485 (1976). doi:10.1038/262484a0
73. A. Mounier, M. Mirazón Lahr, Virtual ancestor reconstruction: Revealing the ancestor of modern humans and Neandertals. *J. Hum. Evol.* **91**, 57–72 (2016). doi:10.1016/j.jhevol.2015.11.002 Medline
74. C. Stringer, The status of Homo heidelbergensis (Schoetensack 1908). *Evol. Anthropol.* **21**, 101–107 (2012). doi:10.1002/evan.21311 Medline
75. D. L. G. Miedzianogora, C. Shipton, M. Pope, Homo heidelbergensis and the origins of The Middle Stone Age: The Kabwe (Broken Hill) lithic assemblage. *Afr. Archaeol. Rev.* **42**, 659–682 (2025). doi:10.1007/s10437-025-09642-8
76. Y. Zhang, A. Biddanda, S. Johnson, C. O'Dushlaine, P. Moorjani, *Trace_software* (Zenodo, 2026); https://doi.org/10.5281/zenodo.21541833.
77. Y. Zhang, A. Biddanda, S. Johnson, C. O'Dushlaine, P. Moorjani, *Trace_pipeline* (Zenodo, 2026); https://doi.org/10.5281/zenodo.20213447.
78. Y. Zhang, A. Biddanda, S. Johnson, C. O'Dushlaine, P. Moorjani, *Trace_data* (Zenodo, 2026); https://doi.org/10.5281/ZENODO.19685110.
79. L. R. Rabiner, A tutorial on hidden Markov models and selected applications in speech recognition. *Proc. IEEE Inst. Electr. Electron. Eng.* **77**, 257–286 (1989).
80. Y. Wong, A. Ignatieva, J. Koskela, G. Gorjanc, A. W. Wohns, J. Kelleher, A general and efficient representation of ancestral recombination graphs. *Genetics* **228**, iyae100 (2024). doi:10.1093/genetics/iyae100 Medline
81. H. Jonsson, P. Sulem, B. Kehr, S. Kristmundsdottir, F. Zink, E. Hjartarson, M. T. Hardarson, K. E. Hjorleifsson, H. P. Eggertsson, S. A. Gudjonsson, L. D. Ward, G. A. Arnadottir, E. A. Helgason, H. Helgason, A. Gylfason, A. Jonasdottir, A. Jonasdottir, T. Rafnar, M. Frigge, S. N. Stacey, O. Th Magnusson, U. Thorsteinsdottir, G. Masson, A. Kong, B. V. Halldorsson, A. Helgason, D. F. Gudbjartsson, K. Stefansson, Parental influence on human germline de novo mutations in 1,548 trios from Iceland. *Nature* **549**, 519–522 (2017). doi:10.1038/nature24018 Medline
82. M. Liang, R. Nielsen, The lengths of admixture tracts. *Genetics* **197**, 953–967 (2014). doi:10.1534/genetics.114.162362 Medline
83. J. Kelleher, A. M. Etheridge, G. McVean, Efficient coalescent simulation and genealogical analysis for large sample sizes. *PLOS Comput. Biol.* **12**, e1004842

(2016). doi:10.1371/journal.pcbi.1004842 Medline
84. B. C. Zhang, A. Biddanda, Á. F. Gunnarsson, F. Cooper, P. F. Palamara, Biobank-scale inference of ancestral recombination graphs enables genealogical analysis of complex traits. *Nat. Genet.* **55**, 768–776 (2023). doi:10.1038/s41588-023-01379-x Medline
85. M. Byrska-Bishop, U. S. Evani, X. Zhao, A. O. Basile, H. J. Abel, A. A. Regier, A. Corvelo, W. E. Clarke, R. Musunuri, K. Nagulapalli, S. Fairley, A. Runnels, L. Winterkorn, E. Lowy, Paul Flicek, S. Germer, H. Brand, I. M. Hall, M. E. Talkowski, G. Narzisi, M. C. Zody, R. E. Mills, T. Rausch, S. Kumar, C. Alkan, F. Hormozdiari, Z. Chong, Y. Chen, X. Yang, J. Lin, M. B. Gerstein, Y. Kai, Q. Zhu, F. Yilmaz, C. Xiao, S. Paul Flicek, H. Germer, I. M. Brand, M. E. Hall, G. Talkowski, M. C. Narzisi, Zody; Human Genome Structural Variation Consortium, High-coverage whole-genome sequencing of the expanded 1000 Genomes Project cohort including 602 trios. *Cell* **185**, 3426–3440.e19 (2022). doi:10.1016/j.cell.2022.08.004 Medline
86. P. Danecek, J. K. Bonfield, J. Liddle, J. Marshall, V. Ohan, M. O. Pollard, A. Whitwham, T. Keane, S. A. McCarthy, R. M. Davies, H. Li, Twelve years of SAMtools and BCFtools. *Gigascience* **10**, giab008 (2021). doi:10.1093/gigascience/giab008 Medline
87. R. K. Dale, B. S. Pedersen, A. R. Quinlan, Pybedtools: A flexible Python library for manipulating genomic datasets and annotations. *Bioinformatics* **27**, 3423–3424 (2011). doi:10.1093/bioinformatics/btr539 Medline
89. International HapMap Consortium *et al*., A second generation human haplotype map of over 3.1 million SNPs. *Nature* **449**, 851–861 (2007). doi:10.1038/nature06258 Medline
89. H. Zhao, Z. Sun, J. Wang, H. Huang, J.-P. Kocher, L. Wang, CrossMap: A versatile tool for coordinate conversion between genome assemblies. *Bioinformatics* **30**, 1006–1007 (2014). doi:10.1093/bioinformatics/btt730 Medline
90. Z. Gao, Y. Zhang, N. Cramer, M. Przeworski, P. Moorjani, Limited role of generation time changes in driving the evolution of the mutation spectrum in humans. *eLife* **12**, e81188 (2023). doi:10.7554/eLife.81188 Medline
91. C. Y. McLean, D. Bristor, M. Hiller, S. L. Clarke, B. T. Schaar, C. B. Lowe, A. M. Wenger, G. Bejerano, GREAT improves functional interpretation of cis-regulatory regions. *Nat. Biotechnol.* **28**, 495–501 (2010). doi:10.1038/nbt.1630 Medline
92. J. M. Mudge, S. Carbonell-Sala, M. Diekhans, J. G. Martinez, T. Hunt, I. Jungreis, J. E. Loveland, C. Arnan, I. Barnes, R. Bennett, A. Berry, A. Bignell, D. Cerdán-Vélez, K. Cochran, L. T. Cortés, C. Davidson, S. Donaldson, C. Dursun, R. Fatima, M. Hardy, P. Hebbar, Z. Hollis, B. T. James, Y. Jiang, R. Johnson, G. Kaur, M. Kay, R. J. Mangan, M. Maquedano, L. M. Gómez, N. Mathlouthi, R. Merritt, P. Ni, E. Palumbo, T. Perteghella, F. Pozo, S. Raj, C. Sisu, E. Steed, D. Sumathipala, M.-M. Suner, B. Uszczynska-Ratajczak, E. Wass, Y. T. Yang, D. Zhang, R. D. Finn, M. Gerstein, R. Guigó, T. J. P. Hubbard, M. Kellis, A. Kundaje, B. Paten, M. L. Tress, E. Birney, F. J. Martin, A. Frankish, GENCODE 2025: Reference gene annotation for human and mouse. *Nucleic Acids Res.* **53**, D966–D975 (2025). doi:10.1093/nar/gkae1078 Medline
93. A. Auton, L. D. Brooks, R. M. Durbin, E. P. Garrison, H. M. Kang, J. O. Korbel, J. L. Marchini, S. McCarthy, G. A. McVean, G. R. Abecasis, S. B. Gabriel, R. A. Gibbs, E. D. Green, M. E. Hurles, B. M. Knoppers, J. O. Korbel, E. S. Lander, C. Lee, H. Lehrach, E. R. Mardis, G. T. Marth, G. A. McVean, D. A. Nickerson, J. P. Schmidt, S. T. Sherry, J. Wang, R. K. Wilson, E. Boerwinkle, H. Doddapaneni, Y. Han, V. Korchina, C. Kovar, S. Lee, D. Muzny, J. G. Reid, Y. Zhu, Y. Chang, Q. Feng, X. Fang, X. Guo, M. Jian, H. Jiang, X. Jin, T. Lan, G. Li, J. Li, Y. Li, S. Liu, X. Liu, Y. Lu, X. Ma, M. Tang, B. Wang, G. Wang, H. Wu, R. Wu, X. Xu, Y. Yin, D. Zhang, W. Zhang, J. Zhao, M. Zhao, X. Zheng, N. Gupta, N. Gharani, L. H. Toji, N. P. Gerry, A. M. Resch, J. Barker, L. Clarke; 1000 Genomes Project Consortium, A global reference for human genetic variation. *Nature* **526**, 68–74 (2015). doi:10.1038/nature15393 Medline
94. J. Choin, J. Mendoza-Revilla, L. R. Arauna, S. Cuadros-Espinoza, O. Cassar, M. Larena, A. M.-S. Ko, C. Harmant, R. Laurent, P. Verdu, G. Laval, A. Boland, R. Olaso, J.-F. Deleuze, F. Valentin, Y.-C. Ko, M. Jakobsson, A. Gessain, L. Excoffier, M. Stoneking, E. Patin, L. Quintana-Murci, Genomic insights into population history and biological adaptation in Oceania. *Nature* **592**, 583–589 (2021). doi:10.1038/s41586-021-03236-5 Medline
95. G. van der Auwera, B. D. O'Connor, *Genomics in the Cloud* (O'Reilly Media, 2020).
96. R. J. Hofmeister, D. M. Ribeiro, S. Rubinacci, O. Delaneau, Accurate rare variant phasing of whole-genome and whole-exome sequencing data in the UK Biobank. *Nat. Genet.* **55**, 1243–1249 (2023). doi:10.1038/s41588-023-01415-w Medline
97. Z. Koenig, M. T. Yohannes, L. L. Nkambule, X. Zhao, J. K. Goodrich, H. A. Kim, M. W. Wilson, G. Tiao, S. P. Hao, N. Sahakian, K. R. Chao, M. A. Walker, Y. Lyu, H. L. Rehm, B. M. Neale, M. E. Talkowski, M. J. Daly, H. Brand, K. J. Karczewski, E. G. Atkinson, A. R. Martin; gnomAD Project Consortium, A harmonized public resource of deeply sequenced diverse human genomes. *Genome Res.* **34**, 796–809 (2024). doi:10.1101/gr.278378.123 Medline
98. S. Rubinacci, O. Delaneau, J. Marchini, Genotype imputation using the Positional Burrows Wheeler Transform. *PLOS Genet.* **16**, e1009049 (2020). doi:10.1371/journal.pgen.1009049 Medline
99. F. M. T. A. Busing, E. Meijer, R. V. A. N. D. E. R. Leeden, Delete-m Jackknife for Unequal m | Statistics and Computing. *Stat. Comput.* **9**, 3–8 (1999). doi:10.1023/A:1008800423698
100. C. M. O'Seaghdha, H. Wu, Q. Yang, K. Kapur, I. Guessous, A. M. Zuber, A. Köttgen, C. Stoudmann, A. Teumer, Z. Kutalik, M. Mangino, A. Dehghan, W. Zhang, G. Eiriksdottir, G. Li, T. Tanaka, L. Portas, L. M. Lopez, C. Hayward, K. Lohman, K. Matsuda, S. Padmanabhan, D. Firsov, R. Sorice, S. Ulivi, A. C. Brockhaus, M. E. Kleber, A. Mahajan, F. D. Ernst, V. Gudnason, L. J. Launer, A. Mace, E. Boerwinckle, D. E. Arking, C. Tanikawa, Y. Nakamura, M. J. Brown, J.-M. Gaspoz, J.-M. Theler, D. S. Siscovick, B. M. Psaty, S. Bergmann, P. Vollenweider, V. Vitart, A. F. Wright, T. Zemunik, M. Boban, I. Kolcic, P. Navarro, E. M. Brown, K. Estrada, J. Ding, T. B. Harris, S. Bandinelli, D. Hernandez, A. B. Singleton, G. Girotto, D. Ruggiero, A. P. d'Adamo, A. Robino, T. Meitinger, C. Meisinger, G. Davies, J. M. Starr, J. C. Chambers, B. O. Boehm, B. R. Winkelmann, J. Huang, F. Murgia, S. H. Wild, H. Campbell, A. P. Morris, O. H. Franco, A. Hofman, A. G. Uitterlinden, F. Rivadeneira, U. Völker, A. Hannemann, R. Biffar, W. Hoffmann, S.-Y. Shin, P. Lescuyer, H. Henry, C. Schurmann, P. B. Munroe, P. Gasparini, N. Pirastu, M. Ciullo, C. Gieger, W. März, L. Lind, T. D. Spector, A. V. Smith, I. Rudan, J. F. Wilson, O. Polasek, I. J. Deary, M. Pirastu, L. Ferrucci, Y. Liu, B. Kestenbaum, J. S. Kooner, J. C. M. Witteman, M. Nauck, W. H. L. Kao, H. Wallaschofski, O. Bonny, C. S. Fox, M. Bochud; SUNLIGHT Consortium; GEFOS Consortium, Meta-analysis of genome-wide association studies identifies six new Loci for serum calcium concentrations. *PLOS Genet.* **9**, e1003796 (2013). doi:10.1371/journal.pgen.1003796 Medline
101. K. P. Schlingmann, M. Kaufmann, S. Weber, A. Irwin, C. Goos, U. John, J. Misselwitz, G. Klaus, E. Kuwertz-Bröking, H. Fehrenbach, A. M. Wingen, T. Güran, J. G. Hoenderop, R. J. Bindels, D. E. Prosser, G. Jones, M. Konrad, Mutations in CYP24A1 and idiopathic infantile hypercalcemia. *N. Engl. J. Med.* **365**, 410–421 (2011). doi:10.1056/NEJMoa1103864 Medline
102. F. Mölder, K. P. Jablonski, B. Letcher, M. B. Hall, P. C. van Dyken, C. H. Tomkins-Tinch, V. Sochat, J. Forster, F. G. Vieira, C. Meesters, S. Lee, S. O. Twardziok, A. Kanitz, J. VanCampen, V. Malladi, A. Wilm, M. Holtgrewe, S. Rahmann, S. Nahnsen, J. Köster, Sustainable data analysis with Snakemake. *F1000 Res.* **10**, 33 (2021). doi:10.12688/f1000research.29032.2 Medline

ACKNOWLEDGMENTS

We thank R. Nielsen, N. Patterson, D. Reich, T. Wang, I. Hariharan and members of the Moorjani and McCoy labs for helpful discussions. We thank Y. Deng for technical support with SINGER, and L. Skov for helpful discussions related to hmmix and IBDmix. We thank N. Patterson, M. Slatkin, E. Kerdoncuff, S. Joseph, M. Tassia, J. Ross-Ibarra and R. McCoy for comments on the manuscript. **Funding:** P. M. was supported by Burroughs Wellcome Fund (Career Award at the Scientific Interface) and P. M. and Y. Z. were supported by the National Science Foundation (CAREER 2338710 to P. M.) S. J. was supported by the NHGRI training grant (5T32HG000047-22). **Author contributions:** Conceptualization: Y.Z., A.B., C.O.D., and P.M.; Data curation: Y.Z., S.A.J., A.B., C.O.D., and P.M.; Formal analysis: Y.Z., A.B.; Funding acquisition: P.M.; Methodology: Y.Z., A.B., and P.M.; Software: Y.Z. and A.B.; Supervision: C.O.D., P.M.; Validation: Y.Z., and P.M.; Writing– original draft: Y.Z., A.B., and P.M.; Writing– review and editing: Y.Z., A.B., S.A.J, C.O.D, and P.M. **Competing interests:** Y.Z., A.B., S.A.J., and P.M. declare no competing interests. C.O.D. is currently employed at insitro, San Francisco, CA 94080, USA. insitro had no involvement in the design or implementation of the work presented here. **Data, code, and materials availability:** No new materials were generated for this study. All resources used in this study are listed and available in tables S1 and

S2. The software implementation of TRACE is available on Zenodo (76). A full pipeline to replicate figures in the manuscript can be found as well (77) and the population-specific archaic ancestry tracts after filtering are available on Zenodo (78).

SUPPLEMENTARY MATERIALS

science.org/doi/10.1126/science.aef8874
Supplementary Text
Figs. S1 to S61
Tables S1, S2, S4 to S12, S14 to S18
References (*78–102*)
Tables S3 and S13

6 February 2026; accepted 25 June 2026
Published online 30 July 2026
10.1126/science.aef8874

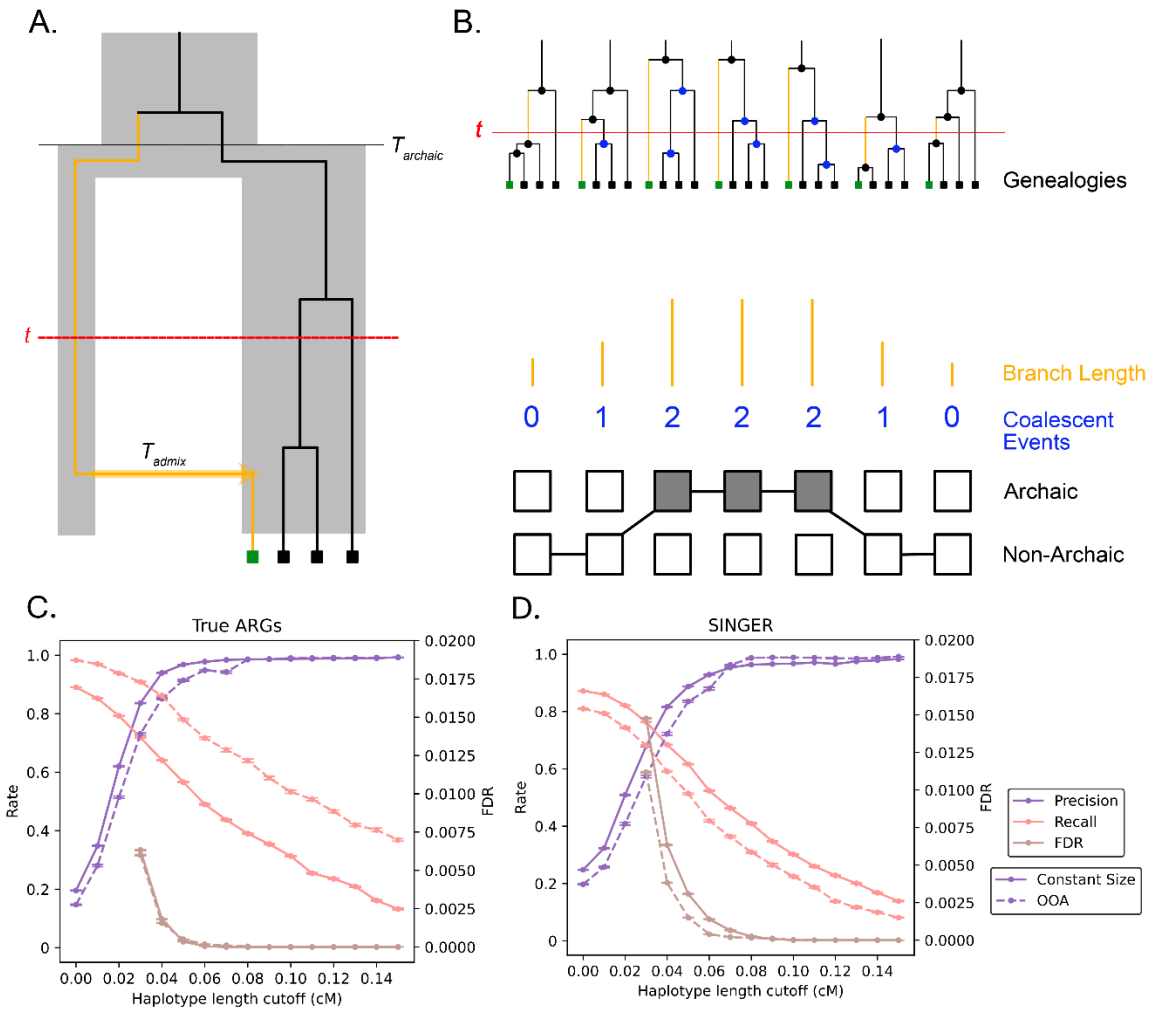

Fig 1. Conceptual overview and validation of TRACE. (**A**) Schematic of local genealogy relating four haplotypes under a demographic scenario of introgression, where introgression affecting the focal haplotype (green dot) creates long branches (orange branch) ancestral to that sample. Specifically, the long branch spans the timepoint of t generations, which is a user-defined timescale to identify archaic events inferred by TRACE, and is shown in the interval between the divergence time of the archaic and modern lineages ($T_{archaic}$) and the time of the admixture event (T_{admix}) in this figure. Individuals without archaic ancestry (black dots) coalesce at the standard rate within the ancestral population - generating coalescent events during the timespan of the orange branch, which is modeled in the single-genealogy emission distribution. Note that time intervals are not drawn to scale. (**B**) Illustration of how the tree sequences are related to emission distributions of the focal branch-lengths and the number of non-focal coalescent events. Coalescent events that are incorporated into the emission distribution for each marginal tree are shown in blue (which occur during the span of the orange branch overlapping t). For simulations of a constant size model (solid line) and an Out-of-Africa (OOA) model (dashed line), we show the Precision (purple), Recall (pink) and False Discovery Rate (FDR, brown) when applying different haplotype length cutoffs (*x*-axis) in TRACE and using (**C**) ground-truth ARGs and (**D**) SINGER-inferred ARGs. Precision and recall fall between 0 and 1, shown as the "Rate" on the left *y*-axis; FDR falls between 0 and 0.02, shown on the right *y*-axis. See also supplementary sections S1 to S3.

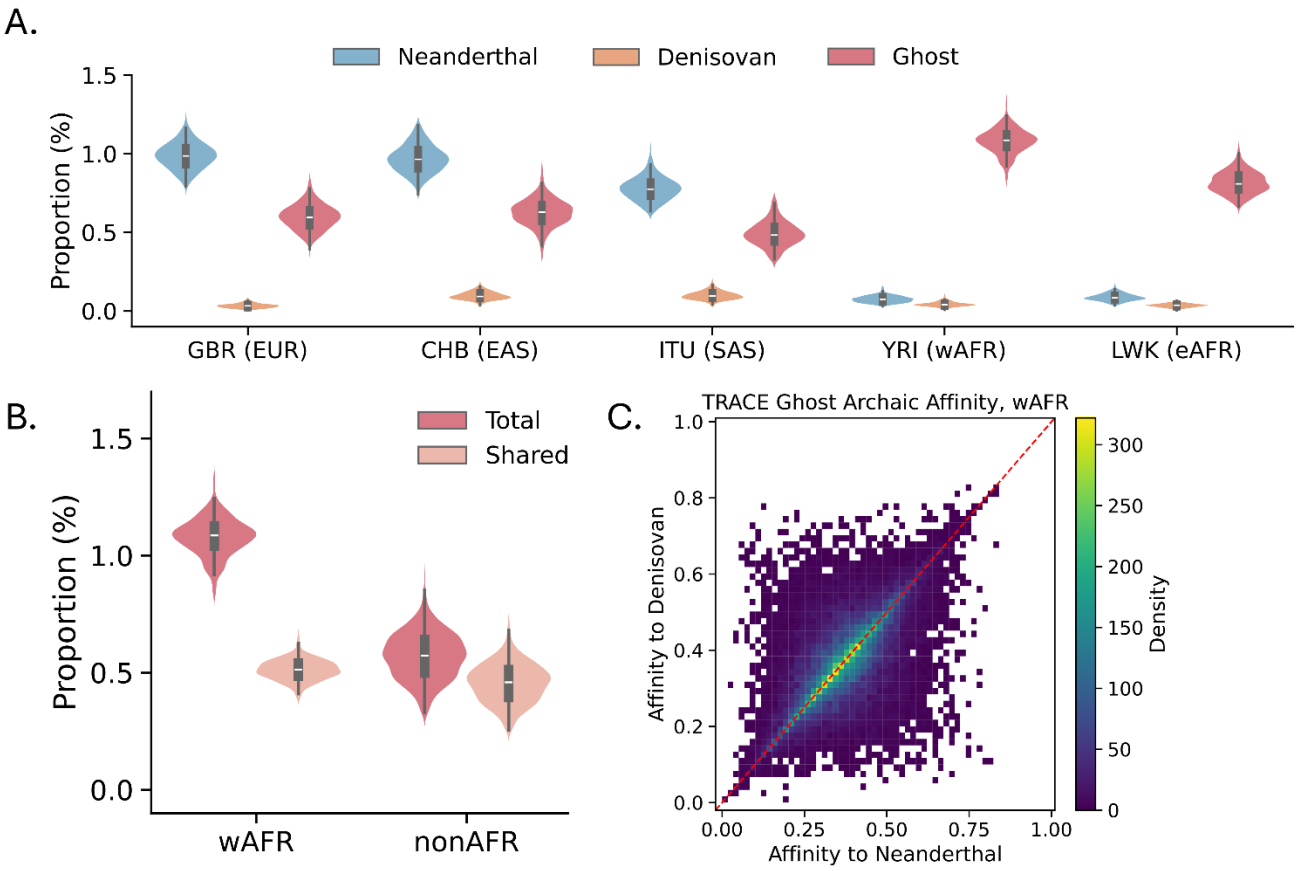

Fig 2. Archaic ancestry in global populations. (A) Proportion of archaic ancestry per genome recovered by TRACE using $t = 15,000$ generations that are > 50 kbp and > 0.05 cM for 1000G populations. Archaic segments are classified as Neanderthal (blue), Denisovan (orange) and Ghost (red) based on allele sharing with sequenced Neanderthal and Denisovan genomes (supplementary section S4.2). (B) The amount of total (dark) and shared (light) ghost archaic ancestry per genome between West Africans and non-Africans. (C) Ghost segments affinity to Neanderthal (*x*-axis) and Denisovan (*y*-axis) genomes in West Africans, calculated as the proportion of derived mutations on the segment shared with Neanderthal and Denisovan sequences.

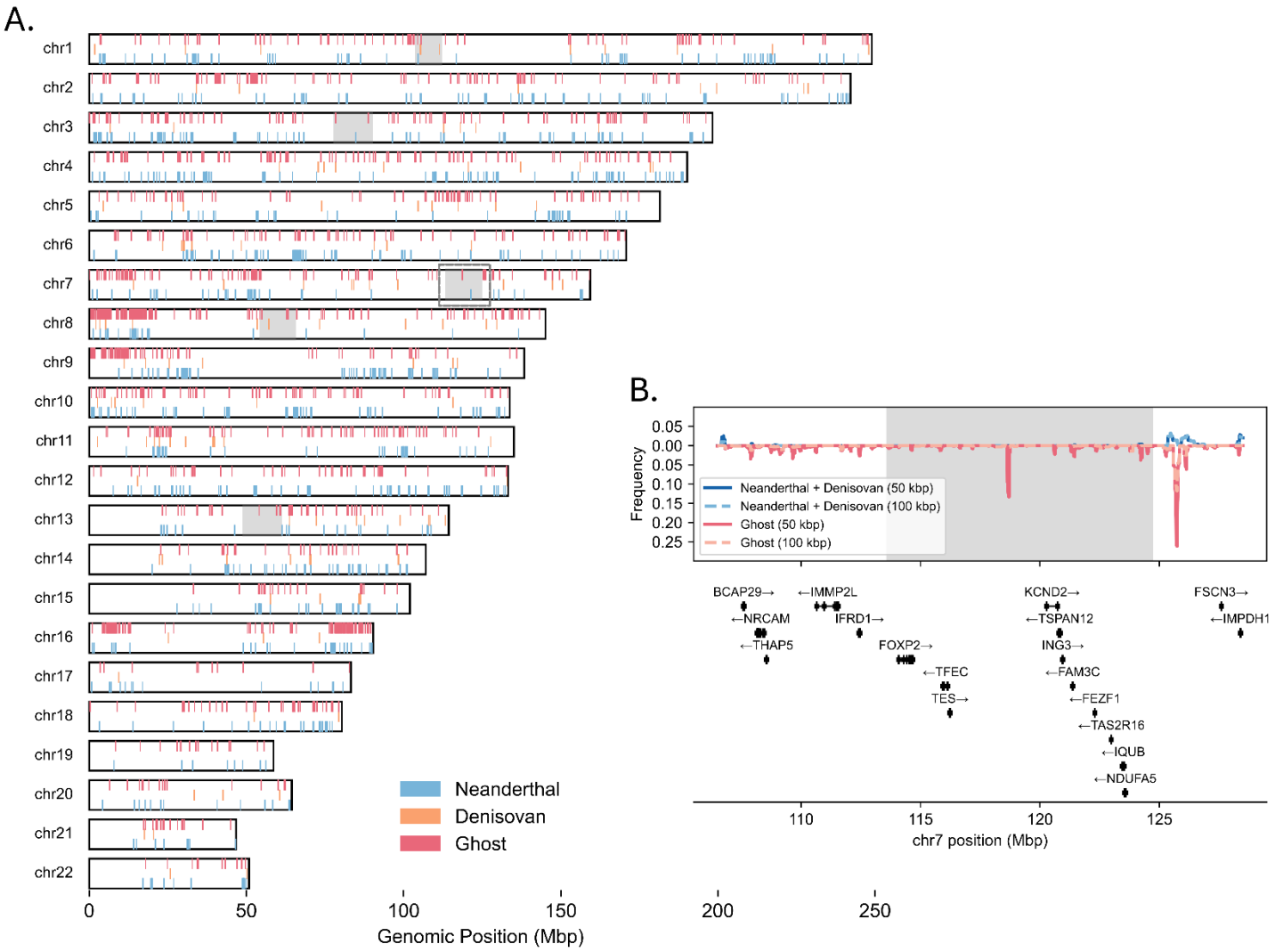

Fig 3. Characterizing the distribution of Archaic ancestry using TRACE. (A) Estimated peaks of archaic ancestry from TRACE—including ghost ancestry—aggregated across all populations. Genomic regions masked as centromeric or genomic regions with no called variants (excluded from ARG inference) are shown in white. Previously estimated deserts of archaic (Neanderthal and Denisovan) ancestry are shown as gray highlights. (B) Frequency of Neanderthal, Denisovan across non-African populations and Ghost ancestry across all populations within the chromosome 7 archaic desert (shown as dashed gray box in (A). The *y*-axis in the top panel reflects the frequency of Neanderthal and Denisovan ancestry, while the *y*-axis in the bottom panel reflects the frequency of Ghost ancestry within the region.

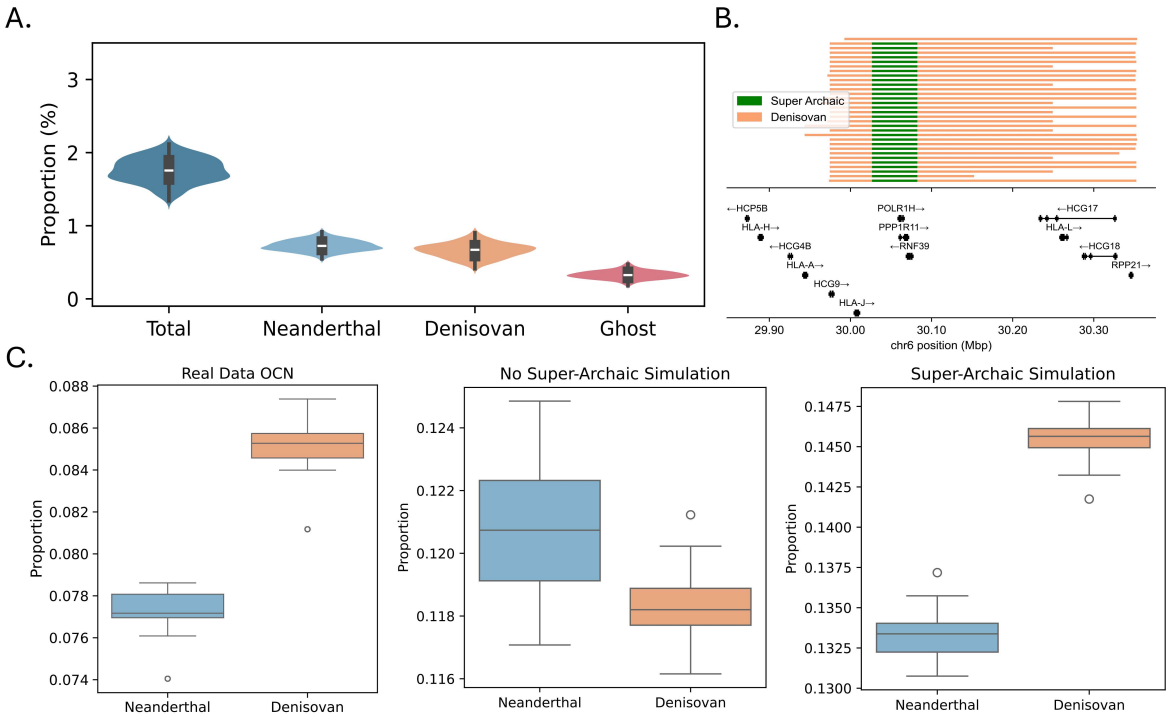

Fig 4. (**A**) Total proportion of Neanderthal, Denisovan, and Ghost ancestries across all sampled Oceanian individuals (**B**) Detected super-archaic ancestry in the MHC region lying on the background of Denisovan ancestry. (**C**) Denisovan segments have a significantly higher proportion of super-deep lineages than Neanderthal segments, a signal reflective of super-archaic ancestry in simulations ($p < 2.2\times10^{-308}, p = 1.00, p< 10^{-36}$ for real data OCN, No Super-Archaic simulation and Super-Archaic simulation respectively; using binomial test).

Recovering signatures of archaic hominin introgression using ancestral recombination graphs

Yulin Zhang, Arjun Biddanda, Sarah A. Johnson, Colm O'Dushlaine, and Priya Moorjani

*Science***Ahead of Print** DOI: 10.1126/science.aef8874